# LEGIBILITY NOTICE

A major purpose of the Technical Information Center is to provide the broadest dissemination possible of information contained in DOE's Research and Development Reports to business, industry, the academic community, and federal, state and local governments.

Although a small portion of this report is not reproducible, it is being made available to expedite the availability of information on the research discussed herein.

RECEIVED BY OSTI JUL 05 1985

LA-UR - 85-1892

CONF-850646--4

MASTER



LA-UR--85-1892

DE85 014135

TITLE CALCULATION OF RF FIELDS IN AXISYMMETRIC CAVITIES

AUTHOR(S) Y. Iwashita



SUBMITTED TO

COMPUMAG
Conference on the Computation of
Electromagnetic Fields

Fort Collins, Colorado
June 3-6, 1985



Los Alamos

Los Alamos National Laboratory
Los Alamos, New Mexico 87545

FORM NO. 836 R4
ST. NO. 2629 5/81

# CALCULATION OF RF FIELDS IN AXISYMMETRIC CAVITIES*

Y. Iwashita†

Abstract – A new code, PISCES, has been developed for calculating a complete set of rf electromagnetic modes in an axisymmetric cavity. The finite-element method is used with up to third-order shape functions. Although two components are enough to express these modes, three components are used as unknown variables to take advantage of the symmetry of the element matrix. The unknowns are taken to be either the electric field components $\mathbf{E} = (E_r, E_\phi, E_z)$ or the magnetic field components $\mathbf{H} = (H_r, H_\phi, H_z)$. The zero divergence condition will be satisfied by the shape function within each element.

## INTRODUCTION

This work was motivated by studies of the disk-and-washer accelerating structure geometry. Because the accelerating mode for these structures does not belong to the lowest passband of possible excitation modes, it is necessary that other modes not overlap the accelerating mode. The modes of greatest concern are those in the $TM_{11}$ passband, which are known to cause beam-deflection problems in some applications.

The most frequently used computer program to evaluate rf cavities is SUPERFISH [1]. SUPERFISH can calculate only symmetric modes in an axisymmetric or two-dimensional geometry. ULTRAFISH [2] was developed to compute the asymmetric modes for such geometries. However, because ULTRAFISH has a numerical difficulty of spurious singularities, it has been difficult to use [3]. PRUD [4] was developed for the same application. The development of PISCES began before URMEL [5] was generally available.

## FORMULATION

The basic equations to be solved are [6,7]

$$\nabla^2 \mathbf{E} + k^2 \mathbf{E} = 0, \quad \mathrm{div}\, \mathbf{E} = 0 \ (\text{in } \Omega) \ , \tag{1}$$

or

$$\nabla^2 \mathbf{H} + k^2 \mathbf{H} = 0, \quad \mathrm{div}\, \mathbf{H} = 0 \ (\text{in } \Omega) \ , \tag{2}$$

where $k^2 = \omega^2 \epsilon\mu$ and $\Omega$ is the entire volume.

Boundary conditions are

$$\mathbf{E} \times \mathbf{n} = 0 \quad \text{or} \quad \mathbf{H} \cdot \mathbf{n} = 0 \tag{3}$$

on electric boundaries $(\Gamma_e)$ for metal surfaces, and

$$\mathbf{E} \cdot \mathbf{n} = 0 \quad \text{or} \quad \mathbf{H} \times \mathbf{n} = 0 \tag{4}$$

on magnetic boundary $(\Gamma_m)$ .

where $\mathbf{n}$ denotes the outward normal on the boundary. Integrating (1) over $\Omega$ after multiplying by $\delta\mathbf{E}$ (virtual electric field) and applying Green's theorem, the following relations must hold for any $\delta\mathbf{E}$

$$\int_\Omega \delta\mathbf{E} \cdot \nabla^2 \mathbf{E} \, dv = -k^2 \int_\Omega \delta\mathbf{E} \cdot \mathbf{E} \, dv \tag{5}$$

or

$$\int_\Gamma [\delta\mathbf{E} (\nabla \cdot \mathbf{E}) + (\nabla \times \mathbf{E}) \times \delta\mathbf{E}] \cdot d\mathbf{S}$$

$$- \int_\Omega [(\nabla \times \delta\mathbf{E}) \cdot (\nabla \times \mathbf{E}) + (\nabla \cdot \delta\mathbf{E})(\nabla \cdot \mathbf{E})] \, dv$$

$$= -k^2 \int_\Omega \delta\mathbf{E} \cdot \mathbf{E} \, dv \ . \tag{6}$$

$$\mathbf{E} \times \mathbf{n} = 0 \qquad \delta\mathbf{E} \times \mathbf{n} = 0 \qquad \text{on } (\Gamma_e) \ , \ \text{and} \tag{7}$$

$$\mathbf{E} \cdot \mathbf{n} = 0 \qquad \delta\mathbf{E} \cdot \mathbf{n} = 0 \qquad \text{on } (\Gamma_m) \tag{8}$$

The second term in surface integration of (6) becomes zero on either $(\Gamma_e)$ or $(\Gamma_m)$ because of the boundary condition of (7) or (8). The first term gives the natural boundary condition. Similar equations can be obtained for H thereafter except for boundary condition differences.

For the element matrix representation,

$$\begin{array}{c} 3\times 1 \\ \mathbf{E} \end{array} = \begin{array}{c} 3\times 3n \\ \begin{bmatrix} \mathbf{N}_\phi & 0 & 0 \\ 0 & \mathbf{N}_r & 0 \\ 0 & 0 & \mathbf{N}_z \end{bmatrix} \end{array} \cdot \begin{array}{c} 3n\times 1 \\ \begin{bmatrix} \mathbf{E}_\phi \\ \mathbf{E}_r \\ \mathbf{E}_z \end{bmatrix} \end{array} \ , \tag{9}$$

where each $\mathbf{N}$ block is $1\times n$ and each $\mathbf{E}$ block is $n\times 1$.

$$\nabla \times \mathbf{E} = \begin{bmatrix} 0 & \partial_z \mathbf{N}_r & \partial_r \mathbf{N}_z \\ \partial_z \mathbf{N}_\phi & 0 & \frac{1}{r}\partial_\phi \mathbf{N}_z \\ \frac{1}{r}\partial_r r \mathbf{N}_\phi & \frac{1}{r}\partial_\phi \mathbf{N}_r & 0 \end{bmatrix} \cdot \begin{bmatrix} \mathbf{E}_\phi \\ \mathbf{E}_r \\ \mathbf{E}_z \end{bmatrix} \ , \tag{10}$$

$$\nabla \cdot \mathbf{E} = \begin{bmatrix} \frac{1}{r}\partial_\phi \mathbf{N}_\phi & \frac{1}{r}\partial_r r \mathbf{N}_r & \partial_z \mathbf{N}_z \end{bmatrix} \cdot \begin{bmatrix} \mathbf{E}_\phi \\ \mathbf{E}_r \\ \mathbf{E}_z \end{bmatrix} \ , \tag{11}$$

where $\mathbf{N}_\phi$, $\mathbf{N}_r$, and $\mathbf{N}_z$ are the shape functions of n parameters for each component, and $\mathbf{E}_\phi$, $\mathbf{E}_r$ and $\mathbf{E}_z$ are the variables for each component. The element matrix equation is

$$\int_\Lambda [(\nabla \times \delta\mathbf{E})^T \cdot (\nabla \times \mathbf{E}) + (\nabla \cdot \delta\mathbf{E})^T (\nabla \cdot \mathbf{E})] \, dv$$

$$= k^2 \int_\Lambda \delta\mathbf{E}^T \cdot \mathbf{E} \, dv \tag{12}$$

*Work supported in part by US Department of Energy

†Accelerator Technology Division, MS H817, Los Alamos National Laboratory, Los Alamos, New Mexico 87545, USA. Permanent address: Institute for Chemical Research, Kyoto University, Kyoto 606, Japan

where $\Delta$ is the element volume, where the symbol T denotes matrix transpose.

To reduce the problem, we shall assume that $E_z$ and $E_r$ depend on $\phi$ only through cos $m\phi$ and that $E_\phi$ depends on $\phi$ only through sin $m\phi$.

Using the same shape function $N$ for each component, and employing (12) for arbitrary $\delta E$, we get the element matrix equation:

$$\begin{bmatrix} F+(1+m^2)P+G & m(2P+G) & m(Q+Q^T) \\ m(2P+G) & F+(1+m^2)P+G & Q+H \\ m(Q+Q^T) & Q^T+H^T & F+m^2P \end{bmatrix} \cdot \begin{bmatrix} E_\phi \\ E_r \\ E_z \end{bmatrix} = k^2 \begin{bmatrix} R & 0 & 0 \\ 0 & R & 0 \\ 0 & 0 & R \end{bmatrix} \cdot \begin{bmatrix} E_\phi \\ E_r \\ E_z \end{bmatrix} \quad (13)$$

where

$$F = \int_\Delta (\partial_r N^T \cdot \partial_r N + \partial_z N^T \cdot \partial_z N)\, r\,dr\,dz, \qquad P = \int_\Delta N^T \cdot N \frac{1}{r}\, dr\,dz \ .$$

$$G = \int_\Delta (N^T \cdot \partial_r N + \partial_r N^T \cdot N)\, r\,dr\,dz, \qquad Q = \int_\Delta N^T \cdot \partial_z N\, dr\,dz \ .$$

$$H = \int_\Delta (\partial_r N^T \cdot \partial_z N - \partial_z N^T \cdot \partial_r N)\, r\,dr\,dz, \qquad R = \int_\Delta N^T \cdot N\, r\,dr\,dz \ .$$

The singularity of $P$ on the axis is not serious because the real divergent term is eliminated by the axial boundary condition. By assembling all element matrices and applying the boundary condition, finally we get the general eigenvalue equation

$$A \cdot x = k^2\, B \cdot x \ . \quad (14)$$

where $A$ and $B$ are symmetric-banded matrices, and $x$ is an eigenvector for the field variables.

## SHAPE FUNCTION AND ZERO-DIVERGENCE CONDITION

The shape function used for each triangular element consists of polynomials up to third order (Fig. 1). The Type 1 element has three compact nodes, where first derivatives are specified together with the value (see Fig. 2a). The shape function is

$$N_1 = \begin{Bmatrix} L_1^2(3 - 2L_1) - 7L_1L_2L_3 \ , \\ L_1^2(z_{21}L_2 - z_{13}L_3) + (z_{13} - z_{21})L_1L_2L_3 \ , \\ L_1^2(r_{21}L_2 - r_{13}L_3) + (r_{13} - r_{21})L_1L_2L_3 \ , \\ \cdots\cdots\cdots\cdots \\ \cdots\cdots\cdots\cdots \\ 27L_1L_2L_3 \end{Bmatrix} \quad (15)$$

$$z_{ij} = z_i - z_j \quad \text{and} \quad r_{ij} = r_i - r_j$$

where $L_i$ is an area coordinate, $z_i$ and $r_i$ are z and r coordinates of the $i^{th}$ vertexes, respectively. A compact node (Type 1 for the top vertex of Fig. 1) is equivalent to three adjacent normal nodes (Type 2 for top vertex of Fig. 1) in terms of specifying the polynomial.[4] Conversion matrix $T_s$ from Type 1 to Type 2 through Type B are generated by MACSYMA to maintain compatibility along the element boundary. That is, if there are only three parameters specified along the side, the fourth one is internally generated by assuming that the variation along the side is of the second order.

$$N \cdot \phi = N \cdot T_s \cdot \psi = N_s \cdot \psi \ . \quad (16)$$

where $N$ is the original shape function of Type 1 or Type C, $N_s$ is the generated shape function, and $\phi$ and $\psi$ are the original and the reduced set of parameters, respectively. Type C (see Fig. 2b) is a regular third-order-polynomial shape function and Types D

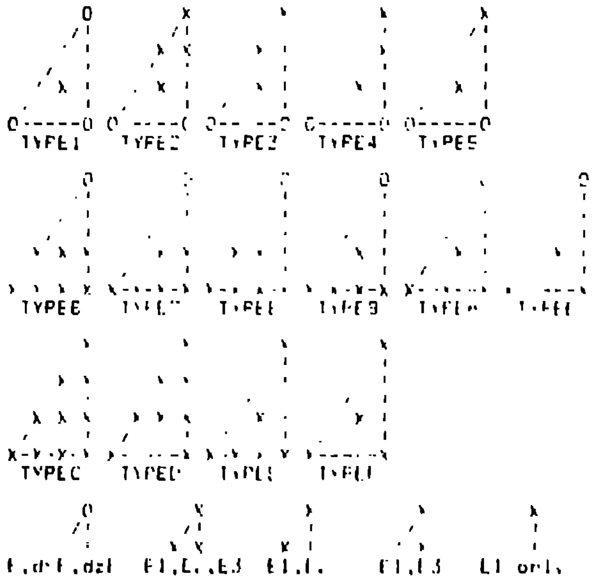

Fig. 1.
Shape functions used in the PISCES program. Symbol O denotes the compact node where three parameters are attached. Symbol X denotes the normal node where only one parameter is attached. The vertex is classed into five types as indicated above.

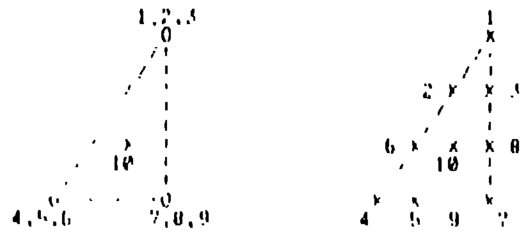

(a) (b)

Fig. 2.
The node numbering scheme: (a) Type 1 element, (b) Type C element.

through F are derived from Type C. The curved boundaries [7] are also available. The centroid value can be eliminated by retaining second-order precision.[8]

Because spurious solutions [6] not satisfying the zero-divergence condition exist, some technique had to be incorporated. There are two methods:
(a) One of the variables at a compact node can be eliminated by the condition

$$\nabla \cdot \mathbf{E} = \frac{m}{r} E_\phi + \frac{1}{r} E_r + \partial_r E_r + \partial_z E_z = 0 \quad . \tag{17a}$$

This condition can be written in matrix form as

$$r \nabla \cdot E = [mN \quad \partial\, rN \quad r\partial\, N] \cdot \begin{bmatrix} E_\phi 1 \\ \partial_z E_\phi 1 \\ \partial_r E_\phi 1 \\ E_r 1 \\ \partial_z E_r 1 \\ \vdots \\ \vdots \\ \partial_r E_z 3 \\ E_\phi 10 \\ E_r 10 \\ E_z 10 \end{bmatrix} = 0 \ . \tag{17b}$$

This can be solved for $\partial_r E_r$ at each vertex of 1 through 3

$$\begin{bmatrix} \partial_r E_r 1 \\ \partial_r E_r 2 \\ \partial_r E_r 3 \end{bmatrix} = \mathbf{S}_v \cdot [\, E_\phi,\ E_r,\ E_z\text{'s except for } \partial_r E_r\text{'s} \,] \ . \tag{18}$$

(b) The centroid-node value $E_\phi$ can be used to impose the integrated zero-divergence condition. [The procedure is similar to (a) above.] The condition in matrix form is

$$\int_\Delta \nabla \cdot \mathbf{E}\, dV = [\ldots \ \ldots \ \ldots] \cdot \begin{bmatrix} E_\phi \\ E_r \\ E_z \end{bmatrix} = 0 \quad . \tag{19}$$

If $m \neq 0$, this can be always solved for centroid value $E_\phi 10$ and we get

$$E_\phi 10 = \mathbf{S}_1 \cdot \begin{bmatrix} E_\phi 1 \\ \partial_z E_\phi 1 \\ \vdots \\ \vdots \\ \partial_r E_z 3 \\ 0 \\ E_r 10 \\ E_z 10 \end{bmatrix} \quad . \tag{20}$$

With $\mathbf{S}_v$ or $\mathbf{S}_1$, we can get the conversion matrix $\mathbf{C}_v$ or $\mathbf{C}_1$:

$$\mathbf{E} = \begin{bmatrix} E_\phi 1 \\ \partial_z E_\phi 1 \\ \vdots \\ \vdots \\ \partial_r E_z 3 \\ E_\phi 10 \\ E_r 10 \\ E_z 10 \end{bmatrix} = \begin{bmatrix} 1 & & & & & & \\ & 1 & & 0 & & & \\ & & \cdot & & & & \\ & 0 & & \cdot & & & \\ 0 & 0 & \cdot & \cdot & 1 & 0 & 0 & 0 \\ \leftarrow & & & S & \cdot & & \rightarrow \\ 0 & 0 & \cdot & \cdot & 0 & 0 & 1 & 0 \\ 0 & 0 & \cdot & \cdot & 0 & 0 & 0 & 1 \end{bmatrix} \cdot \begin{bmatrix} E_\phi 1 \\ \partial_z E_\phi 1 \\ \vdots \\ \vdots \\ \partial_r E_z 3 \\ 0 \\ E_r 10 \\ E_z 10 \end{bmatrix} \tag{21}$$

or $\mathbf{E} = \mathbf{C}_n \cdot \mathbf{y}$, where $\mathbf{y}$ is a reduced component vector, $\mathbf{C}_n$ is $\mathbf{C}_v$ or $\mathbf{C}_1$.

$$\text{Then, shape function} = \begin{bmatrix} \boldsymbol{\phi} & 0 & 0 \\ 0 & \boldsymbol{\phi} & 0 \\ 0 & 0 & \boldsymbol{\phi} \end{bmatrix} \cdot \mathbf{C} \quad , \tag{22}$$

where $\boldsymbol{\phi}$ is one parameter shape function of Type 1 or Type C and $\mathbf{C}$ represents $\mathbf{C}_s$, $\mathbf{C}_s \cdot \mathbf{C}_v$, $\mathbf{C}_s \cdot \mathbf{C}_1$, or $\mathbf{C}_s \cdot \mathbf{C}_v \cdot \mathbf{C}_1$. The element matrix equation becomes

$$\mathbf{C}^T \cdot M \cdot \mathbf{C} \cdot y = k^2\, \mathbf{C}^T \cdot K \cdot \mathbf{C} \cdot y \quad . \tag{23}$$

When $m = 0$, neither the centroid value $E_r$ nor $E_z$ can affect $\int_\Delta \nabla \cdot E\, dV$, and $E_r$ is used to impose $E_r = r\partial_r E_r - r\partial_z E_z$ at the centroid by the same manner as (a). (The centroid node is not the compact node.) No spurious mode can be seen when $m \geq 1$, but when $m = 0$, there are spurious modes because the zero-divergence condition is not sufficiently satisfied in each element. This problem is avoided by using $E_\phi$ and $H_\phi$ components as unknown variables when $m = 0$.

## CORNER SINGULARITY

There is some difficulty at a geometry corner [6] because of the diverging, noncontinuous singularity of the $E_r$ and $E_z$ components. First of all, the point should not be a compact node even for $E_\phi$ and $H_\phi$ solution of $m = 0$ case, because a compact node has smooth value variation and $E_\phi$ has first-order-derivative singularity. One possible solution to this problem is not to maintain the compatibility along the singular boundary: that is, place separate value at the singular point for each element. This problem is still under investigation.

## PROGRAM

The program consists of three parts: the automatic mesh generator NET, the solver PISCES, and the display post processor DISPLAY. The mesh generator NET is still under development using a modified quad tree approach [9]. The input data can be prepared by hand or by using AUTOMESH and LATTICE, which are part of the POISSON group code.

There is a reduced version of PISCES that is 2-D and an axisymmetric version and has an automatic frequency optimization feature suitable for cavity design. The eigenvalue problem is solved by Jennings' method [10], which can simultaneously find any number of eigenvalues and eigenvectors starting with the lowest ones. All modes are obtained including $TE_0$ modes, which cannot be calculated by SUPERFISH and URMEL with simple option. With boundary-condition modification performed by hand, SUPERFISH can calculate $TE_0$ modes. Also, the reduced version DISPLAYO is available for PISCESO. The Q value and the shunt impedance can be evaluated.

## RESULTS

Tables I and II show the eigenfrequencies in a 10 cm radius sphere from the analytic solution, SUPERFISH, URMEL, and PISCES for m = 0 and m = 1. Spurious

TABLE I

COMPARISON OF THE RESULTS FOR 10 cm RADIUS SPHERE WHERE m = 0

| m = 0 | ANALYTIC | SUPERFISH | URMEL | PISCES MAG F 101VF | PISCES ELECTRIC FIELD 101VF | PISCES ELECTRIC FIELD VL... | PISCES ELECTRIC FIELD NONE | PISCES $E_\phi H_\phi$ |
|---|---|---|---|---|---|---|---|---|
| FREEDOM | | 400 | 512 mesh points | 263 | 221 | 201 | 221 | 151 |
| $TM_0$ | 1309 1 | 1309 2 | 1306 7 | 1309 1 | 130[illegible] 5 | 1286 [illegible]<br>x2260 | 130[illegible] 1<br>x2149 0 | 1309 1 |
| $TM_0$ | 2371 0 | 2374 1 | 2364 2 | 2371 1 | 2367 6 | 2365 0 | 2368 5 | 2371 2 |
| $TE_0$ | 2750 0 | (2751 8) | | 2751 4 | 2750 1 | 2750 7 | 2750 [illegible] | 2750 [illegible] |
| $TM_0$ | 2918 5 | 292[illegible] 1 | 291[illegible] 0 | 2919 6<br>x1084 5 | 2916 3<br>x3044 9 | 2927 9 | 2916 1 | 2915 0 |
| $TM_0$ | 3406 8 | 3411 0 | 3385 2 | 3400 5 | 3404 5 | 3411 4 | 3337 5 | 3408 7 |

( ) modified boundary condition
x spurious mode

TABLE II

COMPARISON OF THE RESULTS FOR 10-cm-RADIUS SPHERE WHERE m = 1

| m = 1 | ANALYTIC | URMEL | PISCES | | | |
|---|---|---|---|---|---|---|
| | | | MAG F | ELECTRIC FIELD | | |
| | | | IDIVF | IDIVF | VDIVF | NONE |
| FREEDOM | - - | 1000 | 265 | 219 | 201 | 219 |
| $TM_1$ | 1846.6 | 1848.4 | 1851.9 | 1847.2 | 1822.5 | 1846.9 |
| $TE_1$ | 2144.0 | 2147.6 | 2145.6 | 2144.2 | 2155.6 | 2144.1<br>x2754.5 |
| $TM_2$ | 2892.4 | 2885.7 | 2895.2 | 2893.9 | 2883.9<br>x2903.1 | 2893.7 |
| $TE_2$ | 3334 | 3338.9 | 3338.5 | 3335.8 | 3331.8 | 3335.9 |
| $TM_1$ | 3551.4 | [illegible] | 3554.4 | 3552.6 | 3565.5 | 3554.6 |
| $TE_3$ | 3686.0 | 3686.7 | 3688.8 | 3690.0 | 3674.2 | 3689.6 |

x spurious mode

solutions are marked with an x. In PISCES, there are some options for imposing zero-divergence conditions. One is to use a vertex-node variable, and another is to use a centroid-node value. These options are represented as VDIVF and IDIVF, respectively. Applying both options sometimes makes the system matrix non-positive and unsolvable. The agreement between the analytic value and the results from these codes is reasonable. Figure 3 shows the mesh used and the field pattern for a solution using H as the unknown variable. Figure 4 shows the appearance of a typical system matrix for two cases of m = 0 and a case of m = 1. Only the banded portion of the matrix is stored. One minute of VAX-780 computing time was used for the calculation shown in Table I for $E_\phi$ and $H_\phi$ as unknown variables.

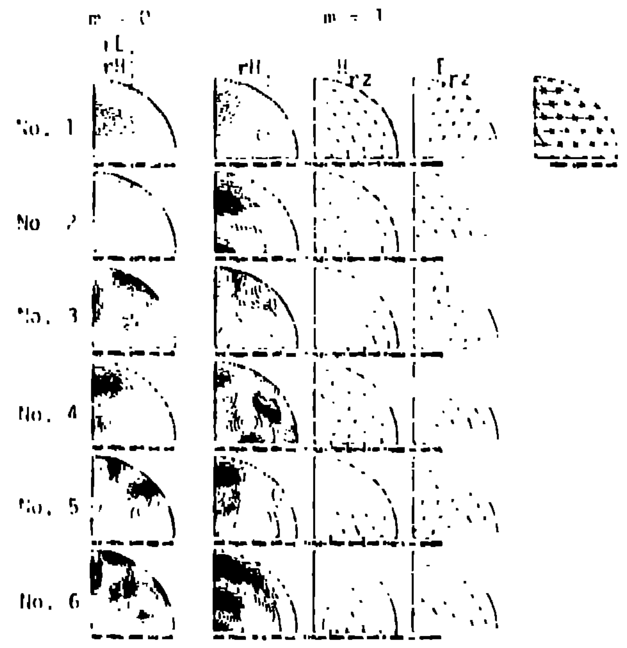


Fig. 3.
A field pattern for a solution using H. The leftmost column shows the m = 0 solution using $E_\phi$ and $H_\phi$.

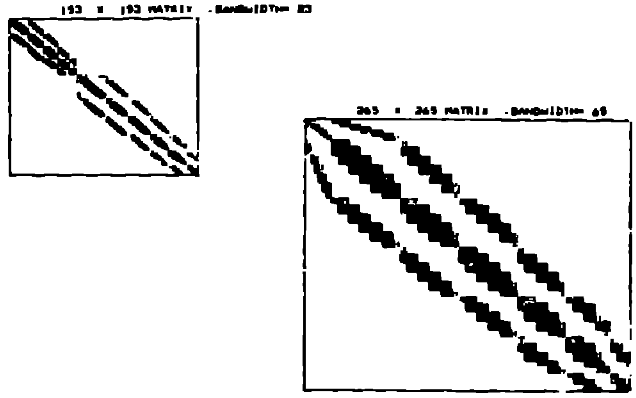

Fig. 4.
Population of system matrices. The m = 0 case is shown on top, and the m = 1 case is on the bottom.


ACKNOWLEDGMENT

The author would like to thank R. K. Cooper, R. L. Gluckstern, R. A. Jameson, S. O Schriber, D. A. Swenson, H. Takekoshi, and T Weiland for their encouragement and discussions.


REFERENCES


[1] K. Halbach and R. F. Holsinger, "SUPERFISH - A Computer Program for Evaluation of RF Cavities with Cylindrical Symmetry," Particle Accelerators 7, 213-222 (1976).

[2] R. F. Holsinger, R. L. Gluckstern, G. N. Minerbo, and K. Halbach, "ULTRAFISH - Generalization of SUPERFISH to m > 1," Proc. 1981 Linear Accelerator Conference, Santa Fe, New Mexico, October 19-23, 1981, Los Alamos National Laboratory report LA-9234 C, 102-107.

[3] Y. Iwashita, "Use of ULTRAFISH and Comparison to Measured Results," Los Alamos National Laboratory technical memorandum AT-DO.82-350, October 18, 1982.

[4] A. G. Daikovsky, Yu I. Portugalov and A. D. Ryabov, "PRUD-Code for Calculation of the Nonsymmetric Modes in Axial Symmetric Cavities," Particle Accelerators 12, 59-64 (1982).

[5] T. Weiland, "On the Computation of Resonant Modes in Cylindrically Symmetric Cavities," Nucl. Instrum. Methods 216, 329-348 (1983).

[6] M. Hara, T. Wada, T. Fukasawa, and F. Kikuchi, "A Three Dimensional Analysis of RF Electromagnetic Fields by Finite Element Method," IEEE Trans. Magn. MAG-19 (6), November 1983.

[7] K. H. Huebner and E. A. Thornton, The Finite Element Method for Engineers, (J. Wiley, New York); and A. R. Mitchell and R. Wait, The Finite Element Method in Partial Differential Equations, (J. Wiley, New York, 1977).

[8] Tsutomu Fujino, Netsudendo to Netsuouryoku (Thermal Conduction and Thermal Stress), Baifukan, Tokyo, Japan (1972), series on Computer Ni Yoru Kozokogakukoza II-4-B (in Japanese).

[9] Mark A. Yerry and Mark S. Shephard, "A Modified Quadtree Approach to Finite Element Mesh Generation," IEEE Computer Graphics & Applications, p. 39, January/February 1983.

[10] FACOM FORTRAN Scientific Subroutine Library, SSL II User's Guide.